Developmentally Regulated Switching of Titin Size Alters Myofibrillar Stiffness in the Perinatal Heart

Christiane A. Opitz, Mark C. Leake, Irina Makarenko, Vladimir Benes, Wolfgang A. Linke

Abstract—Before birth, the compliance of the heart is limited predominantly by extracardiac constraint. Reduction of this constraint at birth requires that myocardial compliance be determined mainly by the heart's own constituents. Because titin is a principal contributor to ventricular passive tension (PT), we studied the expression and mechanics of cardiac-titin isoforms during perinatal rat heart development. Gel electrophoresis and immunoblotting revealed a single, 3.7-MDa, N2BA isoform present 6 days before birth and an additional, also previously unknown, N2BA isoform of 3.5 to 3.6 MDa expressed in the near-term fetus. These large isoforms rapidly disappear after birth and are replaced by a small N2B isoform (3.0 MDa) predominating in 1-week-old and adult rats. In addition, neonatal pig hearts showed large N2BA-titin isoforms distinct from those present in the adult porcine myocardium. By quantitative reverse transcriptase–polymerase chain reaction, developmentally expressed titin-mRNA species were detected in rat heart. Titin-based PT was much lower (≈15 times) in fetal than adult rat cardiomyocytes, and measured PT levels were readily predictable with a model of worm-like chain titin elasticity. Immunofluorescence microscopy showed the extensibility of the differentially spliced molecular spring regions of fetal/neonatal titin isoforms in isolated rat cardiomyofibrils. Whereas the titin-isoform shift by 700 kDa ensures high passive stiffness of the postnatal cardiac myofibrils, the expression of specific fetal/neonatal cardiac-titin isoforms may also have important functions for contractile properties, myofibril assembly or turnover, and myocardial signaling during perinatal heart development. **(*Circ Res*. 2004;94:967-975.)**

Key Words: connectin ■ neonatal ■ rats ■ pigs ■ myocardium

In the developing heart, many myofibrillar proteins show stage-specific isoform expression patterns, with a major isoform switch occurring at approximately the time of birth. In rat ventricle, the β-myosin heavy chain, the predominant fetal isoform, is replaced during early postnatal development by α-myosin heavy chain,[1] and the atrial/embryonic myosin light chain-1, present in fetal ventricles, disappears after birth.[2] At approximately the time of birth, both the cardiac (60% to 70%) and the skeletal (30% to 40%) α-actin isoforms are expressed in rat heart, but in adult rat myocardium, mostly the cardiac α-actin (95%) is present.[3] Similarly, troponin-I and troponin-T isoforms of rat ventricles switch shortly after birth,[4] as do tropomyosin isoforms.[5] All of these changes have a large effect on the contractile properties of the postnatal heart.

In addition, sarcomere proteins not immediately involved in active contractile processes undergo perinatal changes. For instance, the embryonic isoform of a structural protein of the sarcomeric M-line, EH-myomesin, is quickly replaced by adult S-myomesin at approximately the time of birth.[6] Titin is an abundant protein of the sarcomere, which is important in myofibrillar assembly and structure.[7] The giant molecules (3.0 to 3.7 MDa) span half-sarcomeres from the Z-disk to the M-line and are functionally elastic in the I-band.[7–9] As a molecular spring, titin is a main player in determining passive muscle mechanics by developing passive tension (PT) in stretched nonactivated muscle,[7–10] having a high elastic-recoil speed,[11] and contributing to the viscoelastic properties of the muscle.[11,12] Considering the many functions of titin, especially the important mechanical role, it is not unrealistic to expect changes in titin-isoform expression if the global mechanical conditions, such as heart rate, left ventricular dimensions, end-diastolic pressure, and stroke volume, change drastically in the development of the perinatal heart.

Different-length isoforms of titin are generated by alternative splicing of the transcript of a single titin gene.[7] The splicing activity is mainly restricted to the elastic I-band part of titin. In cardiac titin, this elastic part consists of three structurally distinct segments[13]: Ig-domain regions, a PEVK segment rich in proline (P), glutamic-acid (E), valine (V), and lysine (K) residues, and a long unique N2B sequence (see Figure 2A). Differential splicing of cardiac titin occurs in the PEVK segment and the mid-Ig region.[14] In mammalian myocardium, two principal titin isoforms are coexpressed in half-sarcomeres: shorter, stiffer N2B-isoform and longer, more compliant N2BA-isoform.[14] The expression pattern of cardiac-titin isoforms varies from predominantly N2B in

Original received November 14, 2003; revision received January 28, 2004; accepted February 12, 2004.

From the Institute of Physiology and Pathophysiology (C.A.O., M.C.L., I.M., W.A.L.), University of Heidelberg, and European Molecular Biology Laboratory (V.B.), Heidelberg, Germany. Present address for W.A.L. is Physiology and Biophysics Lab, University of Muenster, Muenster, Germany.

Correspondence to Wolfgang A. Linke, PhD, Institute of Physiology and Pathophysiology, University of Heidelberg, Im Neuenheimer Feld 326, D-69120 Heidelberg, Germany. E-mail wolfgang.linke@urz.uni-heidelberg.de

Circulation Research **is available at http://www.circresaha.org** **DOI: 10.1161/01.RES.0000124301.48193.E1**

small adult rodents to predominantly N2BA in bovine atrium, with many large mammals (including humans) expressing intermediate levels of both isoforms.[7,9]

Titin-based PT in the heart may be tuned in two ways: cardiac sarcomeres may express different-length I-band titin, or the N2BA:N2B expression ratio may be modified.[9] When examining titin expression and mechanical function in the perinatal rat heart, we find that fetal titin isoforms of the N2BA-type exist, these isoforms are larger than all titin isoforms previously detected in cardiac tissue, and the expression of titin isoforms of different lengths rapidly adjusts the extensibility and PT of cardiomyofibrils to the prevailing global hemodynamic conditions. Different-size fetal/neonatal titin isoforms expressed in perinatal heart development may also aid sarcomere assembly and turnover and myocardial signaling.

Materials and Methods

Heart Tissue

Heart tissue from Sprague-Dawley rats was obtained from the university's animal house, and pig heart tissue was obtained from local slaughterhouses. The hearts were immediately frozen in liquid nitrogen and stored at −80°C. Frozen human heart tissue was kindly provided by Drs R. Hajjar and F. del Monte (Cardiovascular Research Center, Massachusetts General Hospital, Boston, Mass). All procedures were carried out in accordance with institutional guidelines.

SDS-PAGE and Western Blotting

Agarose-strengthened 2% SDS-polyacrylamide gels, optimized to detect the 3- to 4-MDa titin isoforms with an estimated resolution of ≈100 kDa, were prepared as described.[9,15,16] Immunoblotting was done with a chemiluminescent reaction kit (ECL-system, Amersham Pharmacia) according to standard protocols.

Antibodies

The titin antibodies used have been described before and are indicated in Figures 2 and 5. For additional details, see the online data supplement, available at http://circres.ahajournals.org.

Reverse Transcriptase–Polymerase Chain Reaction

Total RNA was isolated from rat hearts using Trizol (Invitrogen) according to standard protocols. cDNA was synthesized from 1 μg total RNA with the Superscript Choice System for cDNA synthesis (Invitrogen) using random hexamers. Quantitative reverse transcriptase–polymerase chain reaction (RT-PCR) was performed using 25 μL SYBR-Green PCR-Mastermix (Applied Biosystems), 3 μL of 5 μmol/L forward and reverse primer each, 1 μL cDNA template, and 18 μL H_2O and was conducted in an ABI 7000 thermal cycler. The PCR reactions were checked both by melting curve and by gel analysis. Whereas standard curves are widely used for calculating amplification, a recent evaluation of this method[17] showed that it is less erroneous and more practical to directly compare experimental samples against controls. Therefore, the samples were directly compared with one another.

Sample Preparation for Mechanical Measurements

Myofibrils or muscle-cell fragments of adult rat myocardium to be used for force measurements or immunofluorescence (IF) were prepared from triton X-100–skinned tissue as described.[12,15,16]

Immunofluorescence Microscopy

IF measurements on stretched myofibrils were performed with the aid of hydraulic micromanipulators (Narishige) under a Zeiss Axiovert 135 inverted microscope (epifluorescence mode; ×100, 1.4-NA objective) using a Sony color CCD camera.[13,15] For staining protocols, see the online data supplement.

Force Measurements

Skinned cell fragments (diameter, 5 to 8 μm) were suspended between micromanipulator-positioned glass needles attached to a piezoelectric actuator (Physik Instrumented) and a fiber optic–based force transducer (home-built) with nanonewton resolution.[11,16] For details of the stretch protocols, see the online data supplement.

Modeling Titin-Based Stiffness and Stretch-Force Dependence of Epitope Positions

The contribution of the elastic I band titin to myofibrillar passive tension and sarcomeric extensibility was modeled (see the online data supplement) as three worm-like chains (WLCs) acting independently and in series.[8]

An expanded Materials and Methods can be found in the online data supplement, available at http://circres.ahajournals.org.

Results

N2BA and N2B Titin Expression During Perinatal Heart Development

High-resolution gel electrophoresis was performed to detect titin isoforms N2B and N2BA (see domain structure in Figure 2A) in embryonic/fetal and postnatal rat heart (Figure 1A). The distribution and amount of these isoforms during perinatal development and in adulthood were measured in four hearts (at each stage) by analyzing the intensity profiles of titin bands (Figure 1B). The scheme in Figure 1D summarizes the results. Fetal hearts 6 days before birth (e16) expressed almost exclusively a 3700-kDa N2BA-1 isoform. Three days before birth (e19), a 3500- to 3600-kDa N2BA-2 isoform (20%) and the short N2B-isoform (10%) appeared in addition to the N2BA-1 isoform (70%) (also see Figure 1C, left). On the day of birth (1d), the relative proportion of the N2BA-1 isoform had decreased to ≈20%, whereas N2BA-2 and N2B each constituted ≈40% of total T1-titin (also see Figure 1C). Two days after birth (2d), the N2BA-1 isoform disappeared almost completely, and more N2B (55%) than N2BA-2 (40%) was expressed. From 5d to 12d, the amount of N2B-titin rose from 80% to 94%, reaching the level of N2B expression in adult rat heart (Figure 1D). Adult rat heart expresses 93% to 94% N2B-titin, 2% to 3% ≈3400-kDa N2BA-3-titin, and 4% 3200-kDa N2BA-4-titin (Figures 1A and 1D).

The isoform switch was confirmed by Western blotting (Figures 2B and 2C) using the anti-titin antibodies N2B and I25, which stain all cardiac titin isoforms (Figure 2A). Also, the anti-titin antibody MG1 was used, which binds to the N2-A region and thus stains N2BA isoforms only (Figure 2A). The N2BA isoforms expressed in fetal and neonatal rat heart (N2BA-1 and N2BA-2) were larger than the low-abundant N2BA isoforms expressed in adult rat heart (N2BA-3 and N2BA-4, Figure 1D) and in adult human heart (Figure 2B, far right panels). In contrast, the molecular weights of the N2B isoform of fetal/neonatal and adult rat hearts were indistinguishable.

For comparison, we examined titin-isoform expression in the left ventricle of neonatal and adult pig (Figure 1C, right two lanes and intensity profiles). Adult pig heart showed a clear doublet N2BA-titin band. In neonatal pig heart, the proportion of N2BA-titin was increased and additional N2BA isoforms of higher molecular weight than in adult heart were expressed.

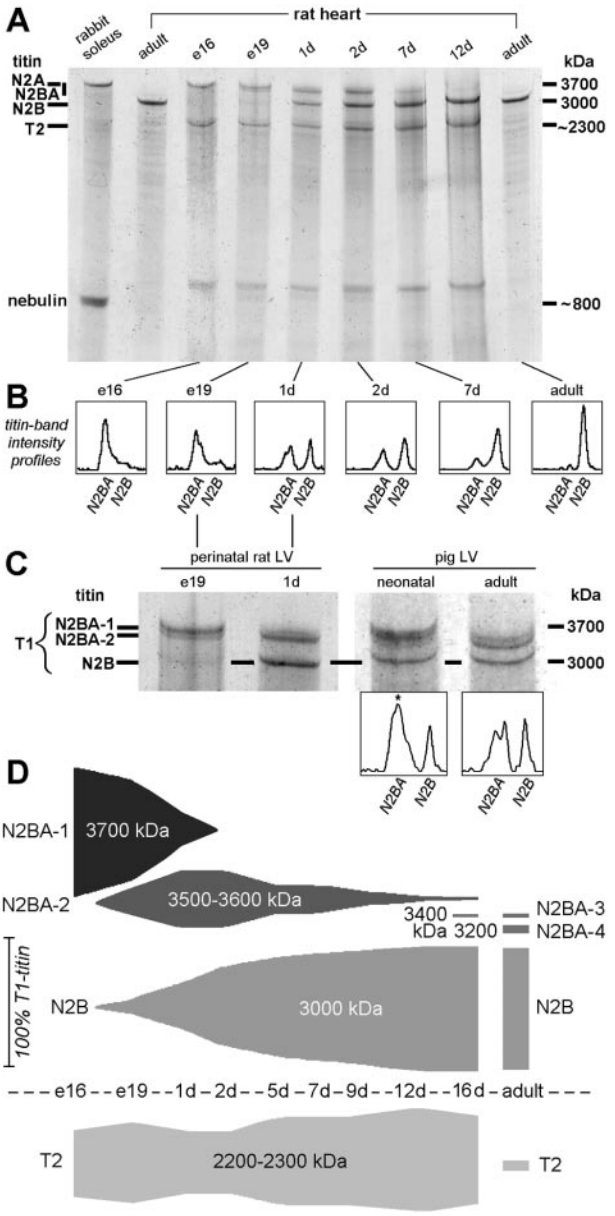

Figure 1. Analysis of titin-isoform expression in developing hearts by 2% SDS-PAGE. Gel lanes (A) and corresponding intensity profiles (B) of T1-titin bands at different time points of rat heart development compared with those of adult rat heart. In adult rabbit-soleus tissue, added for comparison of molecular weight, titin is 3.7 MDa. C, Higher-magnification gel image comparing titin expression pattern of perinatal rat left ventricle (LV) with that of neonatal and adult pig LV. D, Summary scheme showing average proportion of titin isoforms (N2BA+N2B=100%) and their distribution in developing and adult rat heart and titin-degradation band T2. T2 is shown as percentage of N2BA+N2B (=T1). Four hearts were analyzed at each developmental stage. N2BA-1 and N2BA-2 are fetal isoforms; N2BA-3 and N2BA-4 are adult isoforms. e indicates gestational day; d, postnatal day.

Strong T2-Bands May Indicate High Titin-Isoform Turnover During Heart Development

Although all tissue samples were handled identically, samples of developing heart showed very strong T2-titin degradation bands, whereas T2-bands of adult rat myocardium were faint (Figure 1A). The T2-band intensity reached between 50% and 60% of the combined T1-band intensities (N2B+N2BA) at approximately the time of birth and increased to ≈80% at 12d (Figure 1D). This compares to 10% of T2-titin found in adult rat heart. Probably the strong T2 bands in developing heart reflect a high turnover of titin protein. On Western blots, T2-bands were stained with BD6 antibody, which marks titin at the A-band ends, but not with the I-band-titin antibodies used (Figure 2B). With an estimated molecular weight of 2200 to 2300 kDa, T2-titin is likely to contain the 2100-kDa A-band titin[10] plus 100 to 200 kDa of the distal Ig region.

The ≈900-kDa Protein Obscurin Is Upregulated During Heart Development

Strong bands appeared on SDS-polyacrylamide gels of developing rat heart tissue slightly above the nebulin band of rabbit soleus at an estimated molecular weight of 900 kDa (Figure 1A). Because these bands are unlikely to be titin degradation bands (no anti-titin antibody used by us stained the bands; see, for example, Figure 2C), we hypothesized that they could represent either obscurin or some presently unknown, long, cardiac-nebulin isoform. When performing Western blots with the respective antibodies, obscurin-specific antibodies recognized the bands, whereas anti-nebulin antibodies showed no staining (Figure 2B, bottom two rows). Obscurin protein was also detected by immunoblotting in adult rat and human heart (Figure 2B). Whether the high expression level of obscurin—a titin-binding protein[18]—in perinatal heart is related to the expression of fetal titin isoforms is a matter of future study.

Developmental Expression of Titin mRNAs

The levels of titin mRNAs in rat heart tissue at stages e10, e16, 1d, 7d, 16d, and adult were measured by quantitative real-time RT-PCR using the DNA-binding dye SYBR green.[19] Two hearts at each developmental stage were analyzed in quadruplicate.

Because all titin isoforms expressed in the heart (except the truncated novex-3 titin, which was not the subject of this study) contain exons 49 and 50,[20] a primer pair spanning these exons in the rat sequence[21] (Figure 2A) was used to quantify total (N2B+N2BA) cardiac titin. The mRNA level of total cardiac titin stayed more or less the same throughout all developmental stages, except for a small but significant increase on 1d (Figure 3B). Total cardiac titin-mRNA levels were very similar to the levels of N2BA-mRNA. N2BA-mRNA was quantified by using a primer pair that yielded a 110-bp product spanning exons 107 and 108 of the rat-titin N2-A region (Figures 2A and 3A). N2BA-mRNA levels were essentially constant from e10 until adulthood (Figure 3B); only on 1d was a statistically significant increase observable. Similar results were obtained by using another N2BA primer pair that amplified a 71-bp product located on rat-titin exon 108 (Figures 2A and 3A). A primer pair that amplified a 93-bp product spanning rat-titin exons 50 and 219 (Figures 2A and 3A) was used to measure the amount of N2B-mRNA. A great increase in N2B-mRNA was observed from e10 to 16d (Figure 3B). In adulthood, the level of N2B-mRNA expression dropped again. Surprisingly, much less N2B than

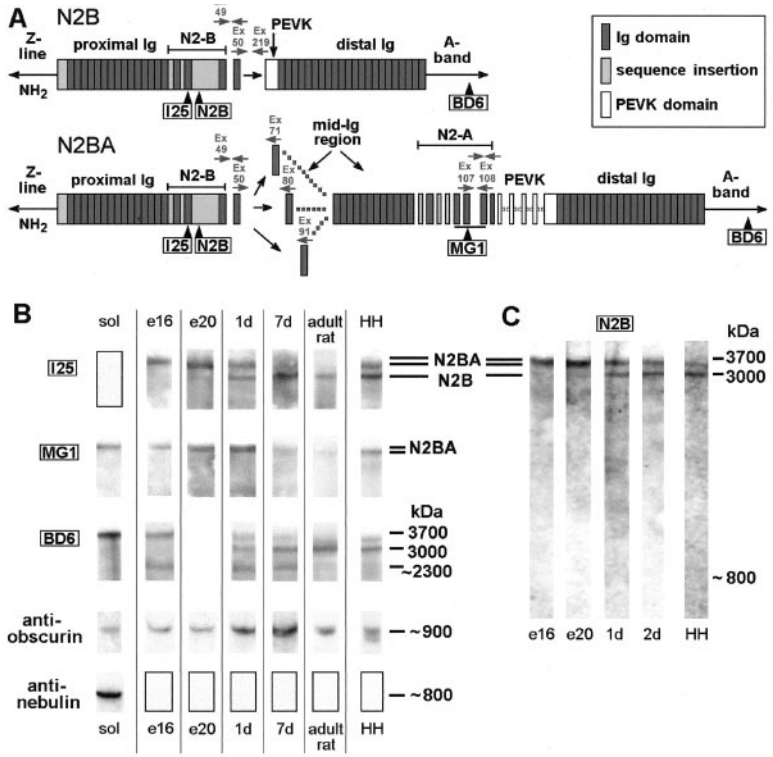

Figure 2. High-molecular-weight proteins in developing rat heart tissues analyzed by Western blotting. A, Domain structure of elastic I-band titin in mammalian heart coexpressing 2 principal isoforms, N2B and N2BA.[14] The epitope locations of the titin antibodies used for Western blotting are indicated (boxes+arrowheads). The positions of the primers used for RT-PCR are indicated by small gray arrows. Ex indicates exon. B, Western blots using sequence-assigned titin antibodies. Lower 2 rows show immunoblots with anti-obscurin and anti-nebulin antibodies. sol indicates adult soleus; HH, adult human heart. C, Whole lanes on Western blot with anti-N2B antibody; no additional high-molecular-weight bands besides T1-titin bands are labeled.

N2BA mRNA was detected in all hearts analyzed at each stage of development (Figure 3B).

Using three primer pairs spanning rat-titin exons 50 to 71, 50 to 80, and 50 to 91 in the variable-length mid-Ig region of N2BA titins (Figure 2A), different N2BA-mRNA splice variants were discriminated (Figure 3C). The lengths of the amplified products, 82, 140, and 121 bp, correspond to the predicted lengths of exon 50 spliced directly to exons 71, 80, and 91, respectively. Detection of N2BA splice variants with all three primer pairs confirms[14,21] a very high activity of alternative splicing in the mid-Ig region.

The three individual N2BA splice variants constituted only a minute fraction of the total N2BA transcripts detected with the primers for the N2-A region (Figure 3). The amount of the product amplified by the primer pair spanning exons 50 to 71 was low before birth, increased at around birth, and decreased again in adulthood (Figure 3C). In contrast, the transcript amplified by the primer pair spanning exons 50 to 80 was abundant before birth and then decreased. The amount of the product amplified by the primers to exons 50 to 91 varied slightly at different stages of heart development and was reduced in the adult heart (Figure 3C).

Titin-Isoform Switching Greatly Increases Myofibrillar Passive Tension in Postnatal Hearts

Force measurements were carried out on nonactivated cardiac myocyte fragments obtained from four adult and four fetal (e16) rat hearts. Force was measured during stepwise stretching of myocyte fragments (skinned myofibril bundles, 5 to 8 μm in diameter), and PT was recorded after 4 seconds of stress relaxation, as demonstrated in Figure 4A. A summary of results (Figure 4B) shows that fetal myocyte fragments developed 15 to 20 times less PT than adult rat hearts at the same sarcomere length (SL).

PT of Cardiomyocytes Is Predictable From the Molecular Weight of Titin Isoforms

The results of the gel-electrophoretic titin analysis were used to predict titin-derived passive force at different stages of perinatal heart development. Predictions of stretch-dependent titin spring force were made by applying a model of titin elasticity encompassing three independent WLCs in series[8] (see the online data supplement). The N2B isoform was modeled as containing 526 residues in the N2-B–unique sequence and 184 PEVK residues.[21] The N2BA-1 and N2BA-2 isoforms were modeled as containing 1995/1216 PEVK residues and 44/30 mid-Ig domains, respectively, in addition to the domains/residues of N2B-titin. The force extension behavior of all titin segments was predicted based on the mechanical properties of individual titin domains measured by single-molecule force spectroscopy.[8] The total force of titin at each given extension was assumed to be the sum of the three force extension relations (Ig regions, PEVK, and N2-B), weighted in proportion to the amount of T1 isoform at the respective developmental stage (Figure 1D).

Modeling results were confirmed by comparing predicted force (Figure 4B, strong, solid lines) to the measured passive force in myocyte fragments. To reconstruct PT, a factor equivalent to the cross-sectional packing density of titin in the myofibril of 2.4×10^9 titin molecules/mm^2, suggested by others,[22,23] was applied. In addition, calculated PT data were multiplied by a scaling factor accounting for the myofibrillar volume density in myocytes. The measured data (mean PT curves) could be well reproduced using a value of 39% and 50% myofibrillar volume in fetal and adult heart tissue,

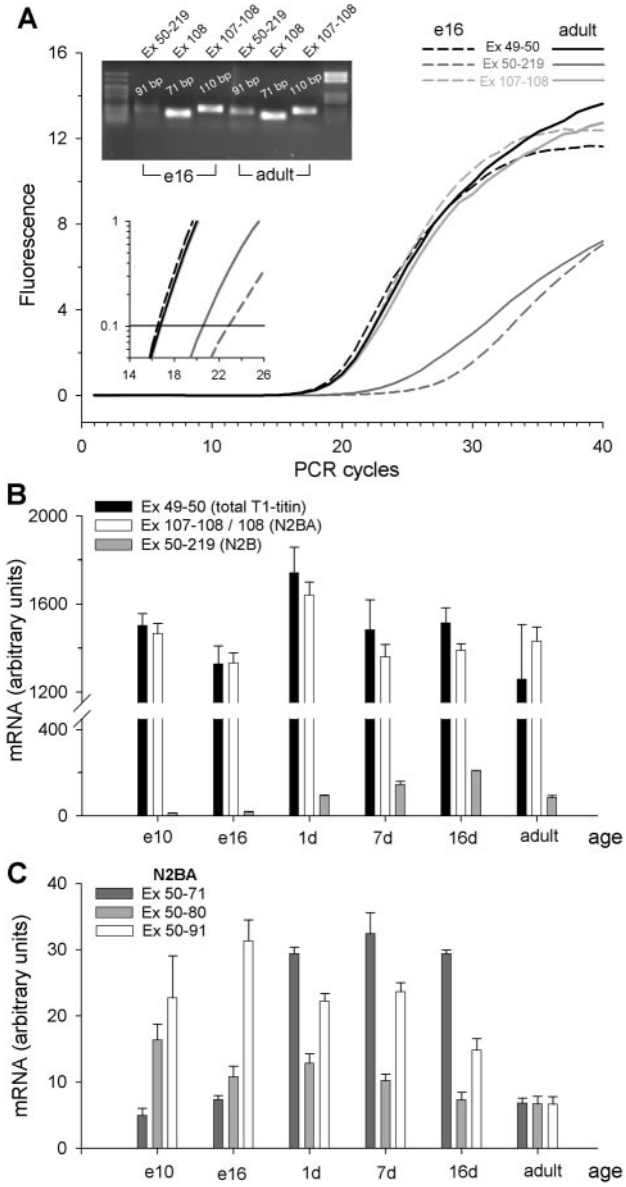

Figure 3. Relative levels of titin-mRNA splice variants from rat heart tissue at stages e10, e16, 1d, 7d, 16d, and adult, measured by real-time RT-PCR using the DNA-binding dye SYBR green. A, Typical amplification curves of exon 49 to 50 (total cardiac titin, N2B+N2BA), exon 50 to 219 (N2B-titin), and exon 107 to 108 (N2BA-titin) rat cDNA (H_2O was used as negative control). Insets, top, Agarose gel to confirm the predicted length of each product; bottom, enlargement (logarithmic scale) of the region where signal intensities crossed the threshold. B, Mean levels and error estimates for titin-exon 49 to 50, 50 to 219, and 107 to 108 mRNA expression. C, Mean levels and error estimates of N2BA-mRNA variants using primer pairs spanning mid-Ig exons 50 to 71, 50 to 80, and 50 to 91 (see Figure 2A).

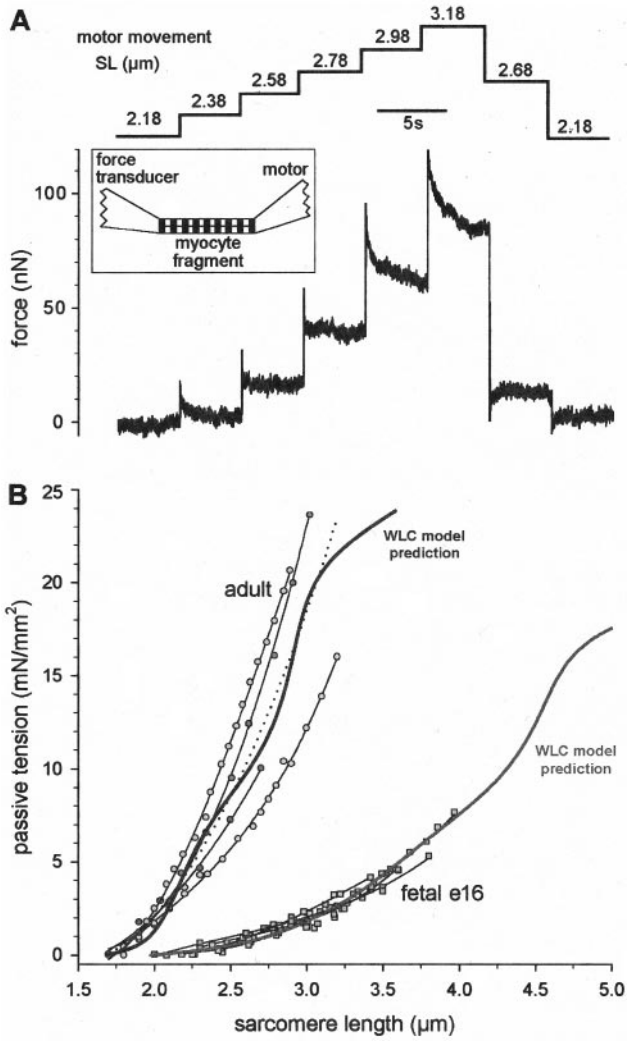

Figure 4. Force measurements on skinned, nonactivated myocyte fragments from fetal (e16) and adult rat heart. A, Stretch protocol (top; SL [micrometer] is indicated) and passive force (lower part) in a fetal (e16) sample. B, Results of PT recordings on 4 fetal (e16) and 4 adult cardiac myocyte fragments. Data points for each sample were fitted by third-order regression. Dotted line is the mean of 4 measurements. Strong solid lines are predictions of PT based on titin-isoform composition, made by applying the WLC model[8] (see the online data supplement). Adult data were reconstituted using 93% N2B isoform content, the remainder taken as N2BA-titin; e16 data were reconstituted using 100% N2BA-1 content. Predictions fitted average measured PT well, assuming 39% and 50% myofibrillar volume in fetal and adult hearts, respectively.

respectively (Figure 4B). These values are in agreement with those found by others in adult and fetal cardiac myocytes.[24]

Extensibility of Differentially Spliced Molecular Spring Regions of Fetal/Neonatal Isoforms

We wanted to know the extensibility of the differentially spliced titin segments (mid-Ig region, PEVK domain) in the I-bands of fetal and neonatal rat heart sarcomeres. Myofibrils were isolated from e16, 1d, and adult rat hearts, and IF microscopy with titin-specific antibodies[13] marking the ends of each segment (Figure 5A) revealed the antibody-epitope positions at different degrees of sarcomere stretch (Figure 5B). The distance between two epitopes measured across the Z-disk was divided by 2 to obtain the Z-disk center to epitope distance. This parameter was plotted against SL in Figures 6A through 6D (symbols).

The epitope positions of all three antibodies moved away from the Z-line with increasing SL, but there were age-dependent and antibody type–dependent differences (Figures 6A through 6D). The I27 epitope moved less in e16 myofi-

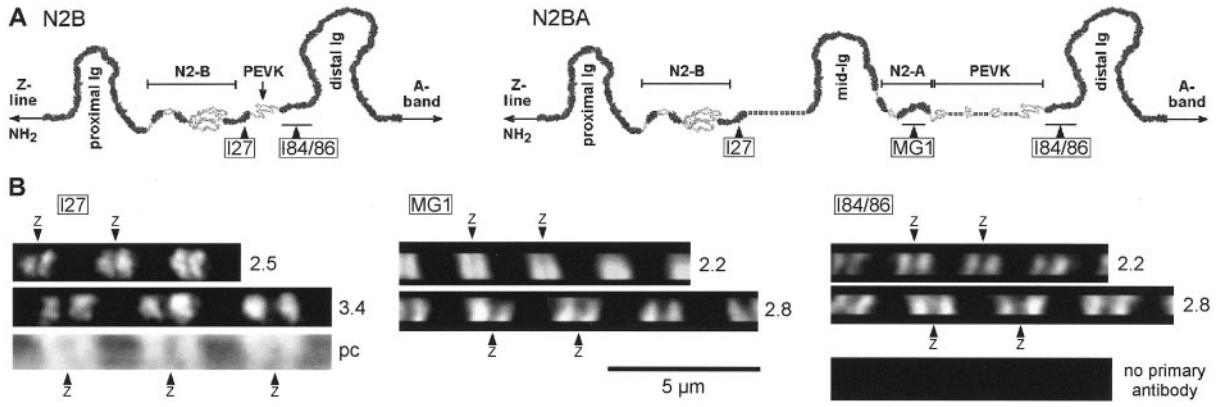

Figure 5. Immunofluorescence microscopy on isolated rat heart myofibrils. A, Schemes of elastic I-band region in cardiac N2B and N2BA isoforms. The anti-titin antibodies used are indicated (boxes+arrowheads). B, Examples of IF images of neonatal (1d) myofibrils extended to different SLs (micrometer, indicated at right of each panel) and stained with the respective primary antibody and Cy3-conjugated secondary antibody. Z indicates Z-line position, determined on phase-contrast (pc) images.

bril expressing nearly 100% N2BA-1 isoform than in 1d samples expressing a mix of isoforms (Figure 6A) over the entire range of SLs investigated (2.0 to 3.5 μm). With MG1, lower mobility of e16 compared with 1d myofibrils was seen only at higher SLs (Figure 6B). The mobility of the I84/86 epitope was not measured in e16 myofibrils, because we did not expect differences to 1d sarcomeres (see below). In adult myofibrils expressing mainly the N2B isoform (which has no mid-Ig region; Figure 5A), we measured the mobility of the PEVK-flanking epitopes I27 and I84/86. Up to the maximum SL studied in adult myofibrils (2.9 μm), the stretch-dependent behavior of both I27 and I84/86 (Figure 6D) was indistinguishable from that in 1d samples.

Again, using previously established information on titin-domain mechanics[8] and the available rat titin-sequence data,[21] we applied the WLC model—but without the need to use any scaling factor—to predict the SL-dependent behavior of titin-antibody epitopes (I27, I84/86, and MG1) in e16, 1d, and adult cardiomyofibrils (curves in Figures 6A through 6D). The approach is explained in the online data supplement. The calculations suggested that the epitope mobility of the I27 antibody should depend on whether the sarcomeres contain N2BA-1, N2BA-2, or N2B titin isoform (Figure 6A). Isoform-related differences in mobility were predicted also for the MG1 antibody, albeit only at higher SLs (Figure 6B), whereas for I84/86, predictions showed almost no difference between the three isoforms (Figure 6C). Thus, the WLC modeling essentially confirmed the measured IF data and suggested that age-dependent differences in antibody mobility are attributable to the presence of different-length titin isoforms in fetal, neonatal, and adult sarcomeres.

The model was then used to determine the extensibility of the mid-Ig and PEVK segments in the N2BA-1, N2BA-2, and N2B isoforms by calculating the distances between the respective epitope mobility curves (Figures 6E and 6F). Extension of the mid-Ig segment of the N2BA isoforms

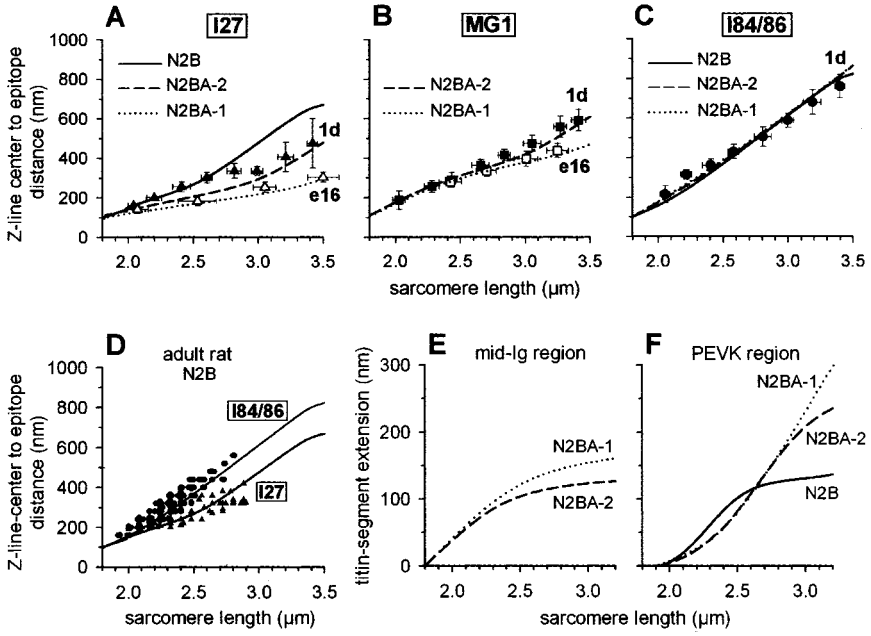

Figure 6. Summarized IF results for fetal (e16), neonatal (1d), and adult rat cardiomyofibrils and WLC modeling of antibody-epitope mobility and titin segment extensibility. A through D, Distance of a given antibody epitope from the center of the Z-disk, plotted against SL. Filled symbols and error bars, 1d-myofibrils; open symbols and error bars, e16-myofibrils; small filled symbols, adult myofibrils. Data are mean±SD (n=5 to 20). Curves are WLC predictions of epitope mobility for individual titin isoforms. E and F, Predicted extensions of differentially spliced titin segments in different isoforms, calculated from the WLC curves in A through D.

began at short SL but then approached a plateau; the segment length near the plateau was longer for N2BA-1 than for N2BA-2 (Figure 6E). Also, the PEVK region of N2BA-1 titin extended more highly than that of the N2BA-2 isoform (Figure 6F), but a plateau was not reached within the SL range studied. In contrast, extension of the PEVK domain of N2B titin leveled out at modest SLs, confirming previous observations.[8,13] Taken together, the IF measurements and WLC modeling revealed an isoform dependency in the mechanical behavior of the differentially spliced I-band titin segments: the N2BA-1 isoform contains the most extensible mid-Ig and PEVK segments, N2BA-2 segments show intermediate extensibility, and N2B segments (PEVK only) show lowest extensibility.

Discussion

Shifts in the ratios between the two main cardiac-titin isoforms, N2B and N2BA, have previously been observed in diseased myocardium. Decreased proportions of N2BA titin were found in a pacing-induced canine model of dilated cardiomyopathy.[25] In end-stage failing human hearts with severe coronary artery disease and in a rat model of chronic myocardial infarction, we reported an increase in N2BA versus N2B isoform.[15] This titin-isoform switching was proposed to help the failing human heart to counteract the increased global stiffening.[15] The cardiac titin-isoform switching observed now in developing rat heart is much more dramatic than the shifts observed in diseased myocardium; within 2 weeks of perinatal development, large 3.7-MDa N2BA isoform is replaced by small 3.0-MDa N2B isoform.

Titin and collagen are known to be the main contributors to passive stiffness in the adult myocardium.[26,27] In the embryonic heart, much less is known about the structures potentially contributing to passive stiffness, ie, intermediate filaments, extracellular matrix material (including collagen), microtubules, or adherence junctions, in addition to titin. The important role of collagen has been explored previously.[28,29] This work now suggests that titin is a principal factor in determining passive stiffness in the perinatal rat heart; because of the isoform shift, the mechanical properties of titin change dramatically within a few days at approximately the time of birth.

The results of the present study thus represent a convincing confirmation of the hypothesis[15,25] that the heart is able to adjust its titin-based passive stiffness by titin-isoform switching (Figure 7). Before birth, when the compliance of the heart is restricted by significant extracardiac constraint,[30] a very long N2BA-1 titin isoform is expressed to keep titin-based PT as low as possible (Figures 7A and 7B, left). At birth, the heart suddenly experiences much-increased filling pressures and significantly reduced extracardiac constraint.[30,31] Therefore, to limit the extensibility and increase titin-based PT, N2B isoform expression is quickly upregulated in the newborn heart; coexpression of N2BA-1, N2BA-2, and N2B isoforms (most likely at the level of the half-sarcomere)[15,32] greatly increases titin-based PT (Figures 7A and 7B, middle). Little more than 1 week after birth, the adult levels of N2B expression are reached; the preponderance of N2B isoforms leads to an additional rise in myofibrillar PT (Figures 7A and 7B, right). Thus, titin-based PT increases between e16 and 12d by a factor of >15. We conclude that, after birth, rapid upregulation of N2B titin acts in concert with increased collagen expression[28,29] to prevent overextension of the rat heart. Furthermore, the titin-isoform switching may impact the heart's active contractile properties; short titin isoforms have been suggested to play a more prominent role in the SL dependence of myofibrillar Ca^{2+} sensitivity than long isoforms.[33] The switch to stiff N2B titin at approximately the time of birth will also increase the proposed contribution of titin elastic recoil to myocardial systolic shortening.[11] Similar to the rat, structural and most likely functional changes in cardiac titin may also take place during perinatal development of larger mammals, such as pigs (Figure 1C).

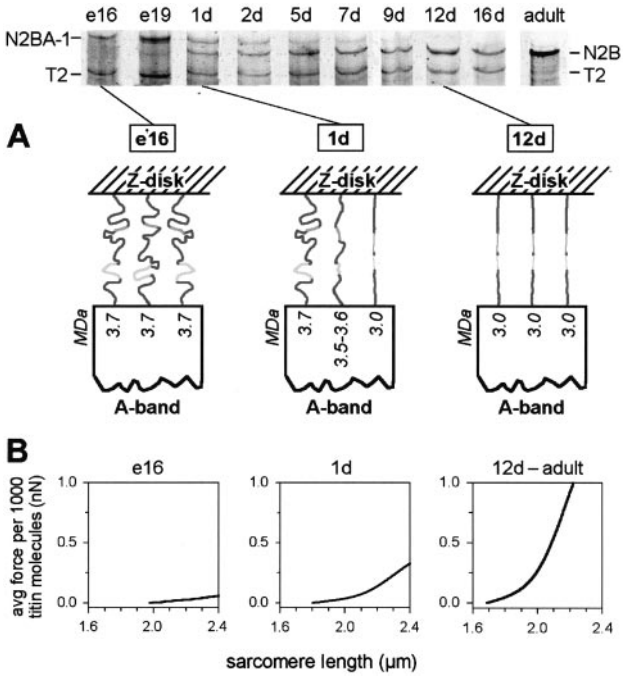

Figure 7. Summary figure showing titin isoform expression in developing rat hearts and consequences for myofibrillar passive stiffness. Top, 2% SDS-PAGE lanes showing perinatal titin-isoform switching. A, Simplistic representation of titin-isoforms in a half-sarcomere at different stages of heart development. B, Predictions of average force per 1000 titin molecules using the WLC model and considering the proportions of N2BA isoforms and N2B isoform at each developmental stage.

How the titin-isoform shift is regulated remains unknown, but our mRNA expression measurements could provide some hints. Because N2B-mRNA and N2B-protein expression correspond well, the developmental expression pattern of the N2B isoform may be regulated at the level of alternative splicing. For the N2BA isoforms, the picture is less clear. Part of this stems from the fact that cardiac titin shows many different N2BA splice pathways (>10 only in the mid-Ig region).[14,21] A plethora of N2BA isoforms is detectable even by SDS-PAGE: fuzzy N2BA bands are observed in neonatal pig heart (Figure 1C) and in diseased (adult) human heart,[15] likely attributable to the expression of many low-abundant N2BA isoforms of varying molecular weight. For the fetal/neonatal and adult rat hearts studied here, the excess of total

N2BA transcript over N2BA protein suggests regulation of N2BA titin at a level downstream of alternative splicing. However, when monitoring three individual N2BA-mRNA splice variants using primers to the mid-Ig region, these variants were low abundant and developmentally regulated (Figure 3C). Could individual splice variants therefore be regulated at the level of alternative splicing?

Indeed, at least a few mRNA splice variants could be regulated only at this level. For example, the product of the primers spanning exons 50 to 71 showed a developmental expression pattern similar to the protein expression levels of the N2BA-2 isoform. A rat N2BA species containing exon 50 spliced to exon 71 has been sequenced[21] and is believed to contain all of the mid-Ig exons between exons 71 and 102. Because one exon usually encodes one Ig domain,[7] ≈30 mid-Ig domains would be present in the N2BA-2 isoform if the detected transcript indeed encoded this isoform. Therefore, we tentatively used a value of 30 mid-Ig domains in the WLC model predictions of N2BA-2 isoform extensibility (Figure 6) and the simulations of titin spring force (Figures 7B, middle).

However, not all splice variants can be regulated only at the level of alternative splicing, because then we would see a better correlation between total N2BA-mRNA and N2BA protein. Therefore, some splice variants are likely to be regulated through other mechanisms, including one or a combination of the following. N2BA splice variants (1) may have a very short half-life (mRNA stability is low), (2) may not be translated into protein, or (3) could show low translational efficiency. Along this line, many recent studies have suggested that the correlation between RNA and protein levels is not always very good.[34]

As an additional factor, at least in developing heart, protein turnover seems to be very high (fetal N2BA isoforms disappear within a few days, and strong T2 degradation bands are found on gels), and relatively more N2BA-mRNA may be needed to express a given amount of protein. In adult rat heart, T2 degradation bands were much less obvious, and high protein turnover is unlikely to be a cause for the extremely low N2BA protein level compared with the N2BA transcript level. Obviously, additional work is needed to elucidate the mechanisms responsible for the mismatch between total N2BA-mRNA and N2BA protein.

Finally, I-band titin has been proposed to be involved also in signaling processes, because it is phosphorylatable[7] and binds to various proteins important for intracellular signaling, energy supply to the contractile apparatus, protein turnover, and folding.[7,35–39] Although speculative at this moment, one can envision that in particular the switch from N2BA-1 to N2BA-2 isoform at approximately the time of birth, as well as the presence of developmentally regulated N2BA isoforms detected by quantitative RT-PCR, play a role far beyond that of mere PT adjustment; these phenomena may well be related to assembly/turnover or signaling processes that optimize perinatal cardiac muscle development.

Acknowledgments

This study was supported by the Deutsche Forschungsgemeinschaft (Li690/6-2; Li690/2-3). W.A.L. was supported by a Heisenberg fellowship from the Deutsche Forschungsgemeinschaft. We thank Rudolf Dussel and Jos de Graaf for expert technical assistance.

References

1. Lompré AM, Nadal-Ginard B, Mahdavi V. Expression of the cardiac ventricular α- and β-myosin heavy chain genes is developmentally and hormonally regulated. *J Biol Chem*. 1984;260:6437–6446.
2. Whalen RG, Sell SM. Myosin from fetal hearts contains the skeletal muscle embryonic light chain. *Nature*. 1980;286:731–733.
3. Carrier L, Boheler KR, Chassagne C, de la Bastie D, Wisnewsky C, Lakatta EG, Schwartz K. Expression of sarcomeric actin isogenes in the rat heart with development and senescence. *Circ Res*. 1992;70:999–1005.
4. Reiser PJ, Westfall MV, Schiaffino S, Solaro RJ. Tension production and thin-filament protein isoforms in developing rat myocardium. *Am J Physiol Heart Circ Physiol*. 1994;267:H1589–H1596.
5. Metzger DM, Michele DE, Rust EM, Borton AR, Westfall MV. Sarcomere thin filament regulatory isoforms: evidence of a dominant effect of slow skeletal troponin I on cardiac contraction. *J Biol Chem*. 2003; 278:13118–13123.
6. Agarkova I, Auerbach D, Ehler E, Perriard JC. A novel marker for vertebrate embryonic heart, the EH-myomesin isoform. *J Biol Chem*. 2000;275:10256–10264.
7. Granzier H, Labeit S. Cardiac titin: an adjustable multifunctional spring. *J Physiol*. 2002;541:335–342.
8. Li H, Linke WA, Oberhauser AF, Carrion-Vazquez M, Kerkvliet JG, Lu H, Marszalek PE, Fernandez JM. Reverse engineering of the giant muscle protein titin. *Nature*. 2002;418:998–1002.
9. Neagoe C, Opitz CA, Makarenko I, Linke WA. Gigantic variety: expression patterns of titin isoforms in striated muscles and consequences for myofibrillar passive stiffness. *J Muscle Res Cell Motil*. 2003;24: 175–189.
10. Tskhovrebova L, Trinick J. Titin: properties and family relationships. *Nat Rev Mol Cell Biol*. 2003;4:679–689.
11. Opitz CA, Kulke M, Leake MC, Neagoe C, Hinssen H, Hajjar RJ, Linke WA. Damped elastic recoil of the titin spring in myofibrils of human myocardium. *Proc Natl Acad Sci U S A*. 2003;100:12688–12693.
12. Kulke M, Fujita-Becker S, Rostkova E, Neagoe C, Labeit D, Manstein DJ, Gautel M, Linke WA. Interaction between PEVK-titin and actin filaments: origin of a viscous force component in cardiac myofibrils. *Circ Res*. 2001;89:874–881.
13. Linke WA, Rudy DE, Centner T, Gautel M, Witt C, Labeit S, Gregorio CC. I-band titin in cardiac muscle is a three-element molecular spring and is critical for maintaining thin filament structure. *J Cell Biol*. 1999;146: 631–644.
14. Freiburg A, Trombitas K, Hell W, Cazorla O, Fougerousse F, Centner T, Kolmerer B, Witt C, Beckmann JS, Gregorio CC, Granzier H, Labeit S. Series of exon skipping events in the elastic spring region of titin as the structural basis for myofibrillar elastic diversity. *Circ Res*. 2000;86: 1114–1121.
15. Neagoe C, Kulke M, del Monte F, Gwathmey JK, de Tombe PP, Hajjar RJ, Linke WA. Titin isoform switch in ischemic human heart disease. *Circulation*. 2002;106:1333–1341.
16. Linke WA, Ivemeyer M, Labeit S, Hinssen H, Rüegg JC, Gautel M. Actin-titin interaction in cardiac myofibrils: probing a physiological role. *Biophys J*. 1997;73:905–919.
17. Peirson SN, Butler JN, Forster RG. Experimental validation of novel and conventional approaches to quantitative RT-PCR data analysis. *Nucleic Acids Res*. 2003;31:e73.
18. Young P, Ehler E, Gautel M. Obscurin, a giant sarcomeric Rho guanine nucleotide exchange factor protein involved in sarcomere assembly. *J Cell Biol*. 2002;154:123–136.
19. Bustin SA. Quantification of mRNA using real-time reverse transcription PCR (RT-PCR): trends and problems. *J Mol Endocrinol*. 2002;29:23–39.
20. Bang ML, Centner T, Fornoff F, Geach AJ, Gotthardt M, McNabb M, Witt CC, Labeit D, Gregorio CC, Granzier H, Labeit S. The complete gene sequence of titin expression of an unusual approximately 700-kDa titin isoform and its interaction with obscurin identify a novel Z-line to I-band linking system. *Circ Res*. 2001;89:1065–1072.
21. Greaser ML, Berri M, Warren CM, Mozdziak PE. Species variations in cDNA sequence and exon splicing patterns in the extensible I-band region of cardiac titin: relation to passive tension. *J Muscle Res Cell Motil*. 2002;23:473–482.

22. Higuchi H, Nakauchi Y, Maruyama K, Fujime S. Characterization of ß-connectin (titin 2) from striated muscle by dynamic light scattering. *Biophys J*. 1993;65:1906–1915.
23. Liversage AD, Holmes D, Knight PJ, Tskhovrebova L, Trinick J. Titin and the sarcomere symmetry paradox. *J Mol Biol*. 2001;305:401–409.
24. Smolich JJ, Walker AM, Campbell GR, Adamson TM. Left and right myocardial morphometry in fetal neonatal and adult sheep. *Am J Physiol*. 1989;257:H1–H9.
25. Wu Y, Bell SP, Trombitas K, Witt CC, Labeit S, LeWinter MM, Granzier H. Changes in titin isoform expression in pacing-induced cardiac failure give rise to increased passive muscle stiffness. *Circulation*. 2002;106: 1384–1389.
26. Linke WA, Popov VI, Pollack GH. Passive and active tension in single cardiac myofibrils. *Biophys J*. 1994;67:782–792.
27. Wu Y, Cazorla O, Labeit D, Labeit S, Granzier H. Changes in titin and collagen underlie diastolic stiffness diversity of cardiac muscle. *J Mol Cell Cardiol*. 2000;32:2151–2162.
28. Engelmann GL. Coordinate gene expression during neonatal rat heart development: a possible role for the myocyte in extracellular matrix biogenesis and capillary angiogenesis. *Cardiovasc Res*. 1993;27: 1598–1605.
29. Carver W, Terracio L, Borg TK. Expression and accumulation of interstitial collagen in the neonatal rat heart. *Anat Rec*. 1993;236:511–520.
30. Grant DA, Fauhere JC, Eede KJ, Tyberg JV, Walker AM. Left ventricular stroke volume in the fetal sheep is limited by extracardiac constraint and arterial pressure. *J Physiol*. 2001;535:231–239.
31. Anderson PA, Manring A, Glick KL, Crenshaw CC Jr. Biophysics of the developing heart, III: a comparison of the left ventricular dynamics of the fetal and neonatal lamb heart. *Am J Obstet Gynecol*. 1982;143:195–203.
32. Trombitas K, Wu Y, Labeit D, Labeit S, Granzier H. Cardiac titin isoforms are coexpressed in the half-sarcomere and extend independently. *Am J Physiol Heart Circ Physiol*. 2001;281:H1793–H1799.
33. Fukuda N, Wu Y, Farman G, Irving TC, Granzier HL. Titin isoform variance and length dependence of activation in skinned bovine cardiac muscle. *J Physiol*. 2003;553:147–154.
34. Greenbaum D, Colangelo C, Williams K, Gerstein M. Comparing protein abundance and mRNA expression levels on a genomic scale. *Genome Biol*. 2003;4:117.
35. Sorimachi H, Kinbara K, Kimura S, Takahashi M, Ishiura S, Sasagawa N, Sorimachi N, Shimada H, Tagawa K, Maruyama K, Suzuki K. Muscle-specific calpain, p94, responsible for limb girdle muscular dystrophy type 2A, associates with connectin through IS2, a p94-specific sequence. *J Biol Chem*. 1995;270:31158–31162.
36. Miller MK, Bang ML, Witt CC, Labeit D, Trombitas C, Watanabe K, Granzier H, McElhinny AS, Gregorio CC, Labeit S. The muscle ankyrin repeat proteins: CARP, ankrd/Arpp and DARP as a family of titin filament-based stress response molecules. *J Mol Biol*. 2003;333:951–964.
37. Ma K, Wang K. Interaction of nebulin SH3 domain with titin PEVK and myopalladin: implications for the signaling and assembly role of titin and nebulin. *FEBS Lett*. 2002;532:273–278.
38. Lange S, Auerbach D, McLoughlin P, Perriard E, Schafer BW, Perriard JC, Ehler E. Subcellular targeting of metabolic enzymes to titin in heart muscle may be mediated by DRAL/FHL-2. *J Cell Sci*. 2002;115: 4925–4936.
39. Bullard B, Ferguson C, Minajeva A, Leake M, Gautel M, Labeit D, Ding L, Labeit S, Horwitz J, Leonard K, Linke WA. Association of the chaperone αB-crystallin with titin in heart muscle. *J Biol Chem*. 2004; 279:7917–7924; published online before print December 4, 2003; 1074/ jbc.M307473200.

Circulation Research
JOURNAL OF THE AMERICAN HEART ASSOCIATION

Developmentally Regulated Switching of Titin Size Alters Myofibrillar Stiffness in the Perinatal Heart

Christiane A. Opitz, Mark C. Leake, Irina Makarenko, Vladimir Benes and Wolfgang A. Linke

Circ Res. 2004;94:967-975; originally published online February 26, 2004;
doi: 10.1161/01.RES.0000124301.48193.E1
Circulation Research is published by the American Heart Association, 7272 Greenville Avenue, Dallas, TX 75231

Print ISSN: 0009-7330. Online ISSN: 1524-4571

Supplementary Information for Opitz et al.

DEVELOPMENTALLY REGULATED SWITCHING OF TITIN SIZE ALTERS MYOFIBRILLAR STIFFNESS IN THE PERINATAL HEART

Expanded Materials and Methods

Heart tissue

Pregnant rats (at different gestational stages), non-pregnant adult and neonatal rats were killed by cervical dislocation and fetal rats were killed by decapitation in accordance with institutional guidelines. The hearts were immediately frozen in liquid nitrogen and stored at -80^{o}C. Whole hearts (prenatal rats) or left ventricles (postnatal rats) were used for further analysis. Elsewhere we reported that freezing does not alter the passive mechanical properties of the samples.[1]

Sodium dodecyl sulphate polyacrylamide-gel electrophoresis and western blotting

2% SDS-PAGE and immunoblotting, optimized for detecting proteins in the megadalton range, were performed as described[2,3] using a Laemmli buffer system.[4] Protein bands were visualised with Coomassie brilliant blue R. Adult rabbit soleus muscle was loaded on each gel to provide known molecular-weight bands for titin (3700 kDa) and nebulin (~800 kDa). Calibration of gel-band intensities and molecular weights was done by generating calibration curves as described in Ref.3. Gels were digitized and densitometric analysis was performed using TotalLab software (Phoretix, Newcastle upon Tyne, UK). Immunoblotting was done with a chemiluminescent reaction kit (ECL system, Amersham Pharmacia) according to standard protocols.[3]

Antibodies

The following titin antibodies were used: MG1 to N2BA-titin[5], and I25[6], I27[7], N2B[6], I84/86[8] and BD6[9] to all cardiac titin isoforms. Anti-obscurin antibody I48/I49[10] and a 1:1 mixture of the antibodies anti-nebulin serine-rich domain and anti-nebulin M176-M181[11] were used for western blotting. We thank Drs. M. Gautel and S. Labeit

for generously providing antibodies. Cy3-conjugated IgG (for IF) and peroxidase-conjugated IgG (for western blotting) served as secondary antibodies.

RT-PCR

Total RNA was isolated from rat-heart tissue at stages e10, e16, 1d, 7d, 16d, and adult using Trizol (Invitrogen) according to standard protocols. cDNA was synthesized from 1µg total RNA with the Superscript™ Choice System for cDNA synthesis (Invitrogen) using random hexamers. RT-PCR primers were designed with a computer program (Primer Express, 2.0). Primer sequences are shown in Table 1. *Rattus norvegicus* sequences[12] were compared with the human genomic sequence of titin (Acc. No. AJ277892),[13] in order to find exon boundaries and the lengths of intermitting introns. Primers were designed across exon boundaries to ensure that no genomic DNA was amplified.

Table 1. Primer pairs used (cf., Fig. 2A and Greaser et al., 2002).[13]

Exons	Sense primer (5'-3')	Antisense primer (5'-3')	GeneBank Acc. No.
Exon 49-50	CCAAGCTCACTGTGGGAGAAA	GCTACTTCCAAGGGCTCAATTC	AF525412
Exon 50-219	CCAACGAGTATGGCAGTGTCA	TGGGTTCAGGCAGTAATTTGC	AF525412
Exon 108	CAAAGCGCATACAGAACATCGT	GTCAAAGGACACTTCACACTCAAAA	AF525411
Exon 107-108	CGGCAGAGCTCAGAATCGA	GTCAAAGGACACTTCACACTCAAAA	AF525411
Exon 50-71	CCAACGAGTATGGCAGTGTCA	ACTACAGGCGGAAAGCTACTAAAAAC	AF525411
Exon 50-80	CCAACGAGTATGGCAGTGTCA	GGAGAGCCACTTATCTTGCATTC	AF525411
Exon 50-91	CCAACGAGTATGGCAGTGTCA	CCCTGGAGCTCGCACTCA	AF525411

Quantitative real-time RT-PCR was performed using 25µl SYBR Green PCR Mastermix (Applied Biosystems), 3µl 5µM forward and reverse primer each, 1µl cDNA template and 18µl H_20. Real-time RT-PCR was conducted in an ABI 7000 thermal cycler. The protocol consisted of 2 min at 50°C, 10 min at 95°C and then 40 cycles of incubation at 95°C for 15 seconds followed by one minute at 60°C. The RT-

PCR primers used all worked with 90-110% efficiency, which allows the reactions to be compared to one another (Invitrogen, real-time qPCR and qRT-PCR protocols). Data acquisition and analysis were performed with ABI Prism 7000 SDS software. Both melting-curve and agarose-gel analysis (Fig.3A in main text) confirmed that the primer pairs used amplified only one product. Whereas standard curves are widely used for calculating amplification, a recent evaluation of this method[14] showed that it is less erroneous and more practical to directly compare experimental samples against controls. In addition it was reported[15] that directly comparing one splice variant to another alleviates the need for an internal control because the control will be cancelled from the ratio between the two splice variants. Therefore, the different titin-mRNA splice variants were directly compared to one another in the present study.

Sample preparation for mechanical measurements

Myofibrils or muscle-cell fragments of adult rat myocardium to be used for force measurements or IF were prepared as described.[16,17] Briefly, thin muscle strips were dissected, tied to thin glass rods and skinned in icecold "rigor" solution (no ATP present) in the presence of 0.5% Triton X-100 for ≥4 hours. To obtain myocyte fragments, the strips were minced and homogenized in rigor solution. Fetal and neonatal heart tissue was homogenized in relaxing buffer (ATP present) by passing through a syringe. All solutions were supplemented with 40 μg/ml protease inhibitor leupeptin to minimize titin degradation.

Immunofluorescence microscopy

IF measurements on stretched myofibrils were performed with the aid of hydraulic micromanipulators (Narishige, Japan) under a Zeiss Axiovert 135 inverted microscope (epifluorescence mode; 100x oil immersion, 1.4NA objective) as described.[6,18] Myofibril images were recorded with an integrating color-CCD camera (Sony), frame grabber, and Scion Image software (NIH, Bethesda, MD).[6] Myofibrils were stretched in relaxing solution containing active-force inhibitor BDM (20mM) and protease inhibitor leupeptin (40μg/ml) at room temperature from slack SL to a desired length, labeled with a primary antibody and, after washout, with Cy3-

conjugated anti-mouse or anti-rabbit IgG. Myofibrils stained with secondary antibody only showed no fluorescence. The analysis of titin antibody-epitope spacing was done as described previously.[6] To detect the Z-lines in each myofibril, IF images were compared with the corresponding phase images.

Force measurements

Skinned cell fragments (diameter, 5-8μm) were suspended between micromanipulator-positioned glass needles attached to a piezoelectric micromotor (Physik Instrumente, Karlsruhe, Germany) and a fibre optic-based force transducer (homebuilt) with nanonewton resolution.[1,2] Data collection and motor control were done with a PC, data acquisition board, and custom-written LabView software (National Instruments, Austin, TX). Force data were related to cross-sectional area inferred from the diameter of the specimens.[19] Passive force of nonactivated myocytes was measured at room temperature in relaxing buffer containing 20mM BDM and 40μg/ml leupeptin. Force was recorded (sampling rate, 2 kHz) in protocols in which specimens were extended step-wise from slack SL. The stretch amplitude per step was 50-300nm/sarcomere; a given stretch step was completed in 10-60ms. Following each step, the specimen was held at a constant SL for at least 4s to wait for stress relaxation. To test for possible shifts of force baseline, myofibrils were released back to slack SL.

Modeling titin-based stiffness and force-dependence of epitope positions based on SDS-PAGE results and mechanical parameters of titin-domain function

The force-extension curve for a given titin isoform in the extensible I-band region of the half-sarcomere was modeled as three wormlike chains (WLCs)[20] acting independently and in series. Evidence suggests that these correspond to segments of tandem-Ig, the PEVK region and the N2B-unique sequence (uN2B).[21] Each was characterized by different persistence and contour lengths such that the total titin extension was given by:

$$X = \sum_{i=1}^{3} x_i \quad .$$

The extension x_i at force F of the i-th spring satisfies (WLC model):

$$F = \frac{k_B T}{L_{pi}} \left(\frac{1}{4(1 - x_i / L_{ci})^2} + \frac{x_i}{L_{ci}} - \frac{1}{4} \right) \quad .$$

The Boltzmann constant is denoted as k_B, the absolute temperature as T, with L_{ci} and L_{pi} the contour and persistence lengths, respectively, of the i-th spring. Solutions for the non-linear equations were found using numerical interpolation. Applying the same approach as Li et al. (2002),[21] unfolding of Ig domains (a rare event *in situ* under normal conditions; Ref. 22) was modeled as either a 2-state process (folded and unfolded) for I1-I15 (the "proximal" domains), with a probability of $P_{prox}=A/(A+B)$ where A and B are force-dependent unfolding and folding rate constants, or as a 3-state process (folded, intermediate and unfolded) for I84-I105 (the "distal" domains), with a probability of $P_{dist}=A_1A_2/(A_1A_2+B_1B_2+A_1B_2)$, with A_1 and B_1 being force-dependent unfolding and folding rate constants between the fully-folded state and an intermediate state, and A_2 and B_2 the equivalent rate constants between the intermediate state and the fully-unfolded state. For N2BA-titin isoforms, the kinetic properties of any Ig domains in the differentially spliced region of I28-I79 (the "mid-Ig" domains; Ref. 13) and in the N2-B/N2-A segments were assumed to be identical to those of the distal Ig domains. The values of parameters used are shown in Table 2. If an Ig domain unfolds, the contour length of the tandem-Ig wormlike chain is assumed to decrease by 4.4 nm, the length of a single folded Ig,[23] with a simultaneous increase in the contour length of the wormlike chain of 32.5 nm.

High resolution SDS-PAGE and western blotting suggested titin in adult rat hearts was almost exclusively the N2B-isoform whereas that in fetal rat hearts (e16) was exclusively a very long N2BA-1-isoform, with molecular weights of 3.0MDa and 3.7MDa, respectively. The difference in molecular weight between the two was assumed to be due to extra insertions of either PEVK or mid-Ig domains in the N2BA-isoform.[12,13] This allowed an estimate for the total Ig-domain insertion given 10-12 kDa for each extra Ig domain, assuming a certain total PEVK length.

Table 2. Parameters used in the prediction of the force-extension relations and antibody-epitope mobility.

N2B-titin isoform (M_w=3.0 MDa)

	A/ s^{-1}	B/ s^{-1}	A_1/ s^{-1}	B_1/ s^{-1}	A_2/ s^{-1}	B_2/ s^{-1}	n	L_p/ nm	L_c/ nm
proximal Ig's	-	-	1.0×10^{-2}	100	3.3×10^{-3}	0.33	15	10	66
distal Ig's	8.0×10^{-5}	1.2	-	-	-	-	22	10	97
mid Ig's (N2-B)	8.0×10^{-5}	1.2	-	-	-	-	4	10	18
PEVK residues	-	-	-	-	-	-	184	0.91	66
uN2B residues	-	-	-	-	-	-	526	0.66	189

N2BA-1-titin isoform (M_w=3.7 MDa)

*	A/ s^{-1}	B/ s^{-1}	A_1/ s^{-1}	B_1/ s^{-1}	A_2/ s^{-1}	B_2/ s^{-1}	N	L_p/ nm	L_c/ nm
proximal Ig's	-	-	1.0×10^{-2}	100	3.3×10^{-3}	0.33	15	10	66
distal Ig's	8.0×10^{-5}	1.2	-	-	-	-	22	10	97
mid Ig's	8.0×10^{-5}	1.2	-	-	-	-	48	10	211
PEVK residues	-	-	-	-	-	-	2179	0.91	784
uN2B residues	-	-	-	-	-	-	526	0.66	189

* The number (n) of extra mid-Ig's has been deduced by assuming that the extra molecular weight after inclusion of additional PEVK of 1995 a.a. for the N2BA-1-titin isoform is due solely to additional Ig domains. Contour lengths for the PEVK and uN2B regions have been calculated on the basis of 0.36nm per residue, with the length for the Ig regions being 4.4nm per domain. As the persistence lengths for distal and proximal Ig segments are considered equal, they can be represented as a single wormlike chain whose contour length is the sum of those for the two separate regions. For the model, mid-Ig's were assumed to have properties equivalent to distal Ig's. All kinetic parameters are taken from data published in Li et al. (2002).[21] Titin sequence information is from Freiburg et al. (2000)[13] and Greaser et al. (2002).[12]
For the N2BA-2-titin isoform (M_w~3.5 MDa), we assumed an additional 30 mid-Ig domains and 1216 PEVK residues, compared to the N2B-isoform.

Passive-tension (T_p) data obtained from skinned myocyte fragments of adult and fetal (e16) rat hearts were modeled. The predicted force-extension relation for a single molecule of each titin isoform was multiplied by a fixed scaling-factor, N, of 2.4×10^9 titin molecules/mm^2, obtained from EM data,[24] and a variable area-factor, α, to account for the proportion of cross-sectional area of the myocyte occupied with myofibrils (a large proportion of cardiac-myocyte volume is non-myofibrillar elements). One sarcomere-length was modeled to consist of two extensible I-band regions of titin and inextensible Z-disk (~200nm) and A-band (~1.6μm) regions. A small variable extension offset X_{offset} was applied to the fit to account for imprecision in SL measurements. The fitting algorithm was written in Matlab using Nelder-Mead Simplex minimization:[25]

$$T_P = \alpha NF\left(X - X_{offset}\right).$$

T_p data from adult rat-heart cells were best fitted using an N2B-titin isoform in the prediction algorithm with an extension offset of -10nm and α=0.50. Best fits for fetal heart (e16) myocyte data were obtained using an N2BA-1-titin isoform with a total PEVK content roughly equivalent to that of the 3.7MDa soleus-muscle titin isoform (an additional 1995 residues compared to the N2B-isoform) and an extra 44 mid-Ig domains, with an extension offset of +20nm and α=0.39. The values of α were consistent with previous estimates for myofibrillar volume fraction estimated from cross-sections of fiber bundles taken from fetal heart,[26] which suggested that no more than ~40% of the total cross-sectional area of a cardiomyocyte is myofibrils, compared with ~50% in adult heart.[27]

Epitope positions for the anti-titin antibodies I27, MG1 and I84/86 were predicted as a function of SL using the same force-extension model, and compared against IF data. The model was used as in Li et al. (2002)[21] to predict the separate extensions of the proximal, mid-Ig, distal, PEVK and uN2B regions as a function of force, and then numerical interpolation was used to generate a functional relationship to SL. The distance of the I27 epitope from the center of the Z-disk was assumed to be

the sum of the extensions of the proximal and uN2B regions plus half the (inextensible) Z-disk width (~100nm). Similarly, the Z-disk-center to MG1-epitope distance was taken as the sum of the extensions of the proximal, uN2B and mid-Ig regions plus half the Z-disk width. The I84/86-epitope distance to the Z-disk center was assumed to be the sum of the extensions of the proximal, uN2B, mid-Ig and PEVK regions plus half the Z-disk width.

Finally, to obtain the extensions of the differentially spliced titin-segments (mid-Ig, PEVK) in the individual isoforms (N2BA-1, N2BA-2, N2B), the modeled antibody epitope-mobility curves were subtracted from one another as follows:
mid-Ig extension: MG1-curve minus I27-curve (e16, 1d myofibrils)
PEVK extension: I84/86-curve minus MG1-curve (e16, 1d myofibrils)
I84/86-curve minus I27-curve (1d, adult myofibrils) = N2B-PEVK.

References

1. Opitz CA, Kulke M, Leake MC, Neagoe C, Hinssen H, Hajjar RJ, Linke WA. Damped elastic recoil of the titin spring in myofibrils of human myocardium. *Proc Natl Acad Sci USA.* 2003;100:12688-12693.
2. Linke WA, Ivemeyer M, Labeit S, Hinssen H, Rüegg JC, Gautel M. Actin-titin interaction in cardiac myofibrils: Probing a physiological role. *Biophys J.* 1997; 73:905-919.
3. Neagoe C, Kulke M, del Monte F, Gwathmey JK, de Tombe PP, Hajjar RJ, Linke WA. Titin isoform switch in ischemic human heart disease. *Circulation.* 2002;106:1333-1341.
4. Tatsumi R, Hattori A. Detection of giant myofibrillar proteins connectin and nebulin by electrophoresis in 2% polyacrylamide slab gels strengthened with agarose. *Anal Biochem.* 1995;224:28-31.
5. Gautel M, Goulding D. A molecular map of titin/connectin elasticity reveals two different mechanisms acting in series. *FEBS Lett.* 1996;385:11-14.

6. Linke WA, Rudy DE, Centner T, Gautel M, Witt C, Labeit S, Gregorio CC. I-band titin in cardiac muscle is a three-element molecular spring and is critical for maintaining thin filament structure. *J Cell Biol.* 1999;146:631-644.
7. Lange S, Auerbach D, McLoughlin P, Perriard E, Schafer BW, Perriard JC, Ehler E. Subcellular targeting of metabolic enzymes to titin in heart muscle may be mediated by DRAL/FHL-2. *J Cell Sci.* 2002;115:4925-4936.
8. Linke WA, Ivemeyer M, Mundel P, Stockmeier MR, Kolmerer B. Nature of PEVK-titin elasticity in skeletal muscle. *Proc Natl Acad Sci USA.* 1998;95:852-857.
9. Whiting A, Wardale J, Trinick J. Does titin regulate the length of muscle thick filaments? *J Mol Biol.* 1989;205:263-268.
10. Young P, Ehler E, Gautel M. Obscurin a giant sarcomeric Rho guanine nucleotide exchange factor protein involved in sarcomere assembly. *J Cell Biol.* 2001;154:123-136.
11. Millevoi S, Trombitas K, Kolmerer B, Kostin S, Schaper J, Pelin K, Granzier H, Labeit S. Characterization of nebulette and nebulin and emerging concepts of their roles in vertebrate Z-discs. *J Mol Biol.* 1998;282:111-123.
12. Greaser ML, Berri M, Warren CM, Mozdziak PE. Species variations in cDNA sequence and exon splicing patterns in the extensible I-band region of cardiac titin: relation to passive tension. *J Muscle Res Cell Motil.* 2002;23:473-482.
13. Freiburg A, Trombitas K, Hell W, Cazorla O, Fougerousse F, Centner T, Kolmerer B, Witt C, Beckmann JS, Gregorio CC, Granzier H, Labeit S. Series of exon skipping events in the elastic spring region of titin as the structural basis for myofibrillar elastic diversity. *Circ Res.* 2000;86:1114-1121.
14. Peirson SN, Butler JN, Forster RG. Experimental validation of novel and conventional approaches to quantitative RT-PCR data analysis. *Nucleic Acids Res.* 2003; 31:e71.
15. Schmittgen TD, Teske S, Vessella RL, True LD, Zakrajsek BA. Expression of prostate specific membrane antigen and three alternatively spliced variants of PSMA in prostate cancer patients. *Int J Cancer.* 2003;107:323-329.

16. Linke WA, Ivemeyer M, Olivieri N, Kolmerer B, Rüegg JC, Labeit S. Towards a molecular understanding of the elasticity of titin. *J Mol Biol.* 1996;261:62-71.
17. Kulke M, Fujita-Becker S, Rostkova E, Neagoe C, Labeit D, Manstein DJ, Gautel M, Linke WA. Interaction between PEVK-titin and actin filaments: origin of a viscous force component in cardiac myofibrils. *Circ Res.* 2001b;89:874-881.
18. Kulke M, Neagoe C, Kolmerer B, Minajeva A, Hinssen H, Bullard B, Linke WA. Kettin a major source of myofibrillar stiffness in Drosophila indirect flight muscle. *J Cell Biol.* 2001a;154:1045-1057.
19. Linke WA, Popov VI, Pollack GH. Passive and active tension in single cardiac myofibrils. *Biophys J.* 1994;67:782-792.
20. Marko JF, Siggia E. Stretching DNA. *Macromolecules.* 1995;28:209-212.
21. Li H, Linke WA, Oberhauser AF, Carrion-Vazquez M, Kerkvliet JG, Lu H, Marszalek PE, Fernandez JM. Reverse engineering of the giant muscle protein titin. *Nature.* 2002;418:998-1002.
22. Minajeva A, Kulke M, Fernandez JM, Linke WA. Unfolding of titin domains explains the viscoelastic behavior of skeletal myofibrils. *Biophys J.* 2001;80:1442-1451.
23. Pfuhl M, Gautel M, Politou AS, Joseph C, Pastore A. Secondary structure determination by NMR spectroscopy of an immunoglobulin-like domain from the giant muscle protein titin. *J. Biomolec. NMR.* 1995;6:48-58.
24. Liversage AD, Holmes D, Knight PJ, Tskhovrebova L, Trinick J. Titin and the sarcomere symmetry paradox. *J Mol Biol.* 2001;305:401-409
25. Nelder JA, Mead R. A simplex method for function minimization. *Computer J.* 1965;7:308-313.
26. Smolich JJ, Walker AM, Campbell GR, Adamson TM. Left and right myocardial morphometry in fetal neonatal and adult sheep. *Am J Physiol.* 1989;257:H1-9.
27. Sommer JR, Johnson EA. Ultrastructure of cardiac muscle. In: Burns R, eds. *Handbook of Physiology. The Cardiovascular System*, Sec. 2, Vol. 1. American Physiological Society, Bethesda, MD; 1979:113-186.